2021

Evaluation of Heat Pumping and Waste Heat Recovery for Battery Electric Vehicle Thermal Management

Tyler Shelly
Purdue University, United States of America, tshelly@purdue.edu

Justin Weibel

Davide Ziviani

Eckhard Groll

Evaluation of Heat Pumping and Waste Heat Recovery for Battery Electric Vehicle Thermal Management

Tyler J. SHELLY[1]*, Justin A. WEIBEL[1], Davide ZIVIANI[1], Eckhard A. GROLL[1]

[1]School of Mechanical Engineering, Cooling Technologies Research Center, Herrick Laboratories, Purdue University
West Lafayette, IN, USA
tshelly@purdue.edu (316)-212-3280

* Corresponding Author

ABSTRACT

Due to increasing regulation on emissions and shifting consumer preferences, the wide adoption of battery electric vehicles (BEV) hinges on research and development of technologies that can extend system range. This can be accomplished either by increasing the battery size or via more efficient operation of the electrical and thermal systems. This study evaluates the range performance of a BEV integrated thermal management system (ITMS) with heat pumping and waste heat recovery across a range of ambient conditions (-20 °C to 40 °C) and cabin setpoints (18 °C to 24 °C). A dynamic ITMS modelling framework for a long-range electric vehicle is established with comprehensive sub models for the operation of the drive train, power electronics, battery, vapor compression cycle components, and cabin conditioning. This modelling framework is used to construct a baseline thermal management system. The waste heat recovery (WHR) system is compared to the baseline and shown to offers significant benefit in terms of driving range for long-range BEV drive cycles in terms of system range and transient response.

1. INTRODUCTION

As the vehicle fleet continues to electrify, the thermal management of battery electric vehicles (BEV) has significant on their operating range, especially in extreme climate conditions. Traditional heat sources available for cabin heating from internal combustion engines (ICE) are missing in BEVs, and furthermore, the replacement electrical components must adhere to tight thermal tolerances. The active management of these components is the focus of this study. Each component will be introduced in the context of its active thermal management strategy, impact on system range, and unique opportunities for ITMS architecture enhancements, followed by a review of recent literature that focuses on EV thermal systems including the power electronics, cabin environment, battery conditions, and their optimization.

Electric vehicle batteries and their associated cooling systems have been extensively studied in the literature, as previously exhaustively reviewed in Refs. [1] [2]. The goals of these past studies typically are to optimize existing cooling methods, establish alternate cooling methods, and investigate battery cell architectures. EV battery cooling methods investigated in the literature include air cooling, liquid cooling, direct refrigerant cooling, and immersion cooling [1] [2]. Air-cooled batteries are typically found in shorter range electric vehicles. Longer range BEVs typically implement liquid cooling due to more favorable heat transfer characteristics that allow for a denser cooling solution. In the case of a direct liquid cooling solution, coolant is brought as close as possible to the battery for optimal heat transfer performance while an indirect solution places a cold plate along the bottom of the entire battery system's length while providing fins to interface with the battery. Direct refrigerant systems bring two phase refrigerants to the battery via a cold plate and manifold system, like a direct liquid cooling solution, and evaporate the refrigerant. A more uniform and higher capacity cooling are associated with two-phase flow of the refrigerant across the battery cold plate. Currently, these two-phase cooling methods have limited implementation in the consumer market [1] [2]. The current study focuses on ITMS architectures having a secondary loop, indirect liquid cooling system for the battery. Analysis across a wide range of ambient conditions to examine their performance in heating and cooling modes has been identified as a gap in past research [1].

Heating, ventilation, and air conditioning (HVAC) solutions are critical for all vehicles to ensure consumer comfort across a wide range of ambient conditions. EV cabin cooling solutions mirror those for internal combustion engine

(ICE) vehicles [3]. Typical cooling solutions include the use of a traditional vapor compression cycle (VCC). The design of EV cabin heating systems diverge from ICE vehicles. In ICE vehicles, the large amount of waste heat available from the engine can meet the heating needs of the vehicle even in extremely cold environments. Electric vehicles must rely on alternate forms of heating, such as direct electric heating from positive temperature coefficient (PTC) heaters, heat pumping, fuel-based heaters, or the use of recovered waste heat from the power electronics. Direct electric heating is intrinsically limited to coefficient of performance (COP) of 1, making it a large parasitic draw on the EV traction battery. A heat pump (HP) reverses the flow inside of a typical VCC and rejects heat to the cabin while taking in heat from the ambient. HP heating systems typically suffer from a lack of heating capacity at extremely low ambient temperatures. Waste heat recovery is the use of waste heat produced by the power electronics for either battery or cabin heating. The last remaining components requiring thermal management in an EV are the electric drive systems. These components typically include the auxiliary power module (APM), traction power inverter module (TPIM), and electric motor (EM) [4] [5], which are typically air or liquid cooled [6] [7].

This work first outlining of a comprehensive EV model applicable for evaluation of EV thermal management systems. Then, two EV thermal management systems (TMS) are constructed in this modeling framework and their control methodologies are introduced. Lastly, the range performed for the two systems are presented and discussed.

2. THERMAL MANAGEMENT SYSTEMS ARCHITECTURES, CONTROL, AND MODELING

2.1 Baseline Thermal Management System

In a previous work [8], the authors established a baseline TMS having the most typical solutions for cabin HVAC, battery thermal management, and electronics cooling for a long-range BEV. The baseline TMS, detailed in Figure 1a has a standard vapor compression cycle (VCC) that is used for direct cabin cooling and indirect battery cooling via a secondary water-glycol loop. Superheated R134a refrigerant is compressed across a parameterized scroll compressor and then condensed via heat exchange with ambient air. The refrigerant flow splits and can expand across two expansion valves. The first valve (V1) leads to the cabin heat exchanger (HX) while the second valve (V2) leads to the battery HX and cools a secondary water-glycol flow loop that conditions the battery through a cold plate attached to the battery. This secondary pumped loop has an electric heater to heat the battery to an appropriate setpoint in cold conditions, such as an event where the vehicle is cold soaked overnight. The system electronics are cooled through an additional pumped water-glycol loop which reject heat to the air via the radiator [8]. Cabin and battery heating are performed via heat sources interfaced with the water-glycol coolant flow for the battery and a secondary liquid-to-air heat exchanger for the cabin environment. The battery is sized to provide 100 kWh of capacity.

The system control logic follows typical component control schemes using proportional integral controllers. A variable-speed compressor is assumed to be electrically driven rather than belt driven and controls for the inlet cabin air temperature across the cabin HX. System pumps and fans are controlled to set appropriate battery and cabin mean temperatures, respectively. The two expansions valves for the cabin and battery plate heat exchanger control the evaporator superheat and battery inlet temperature, respectively.

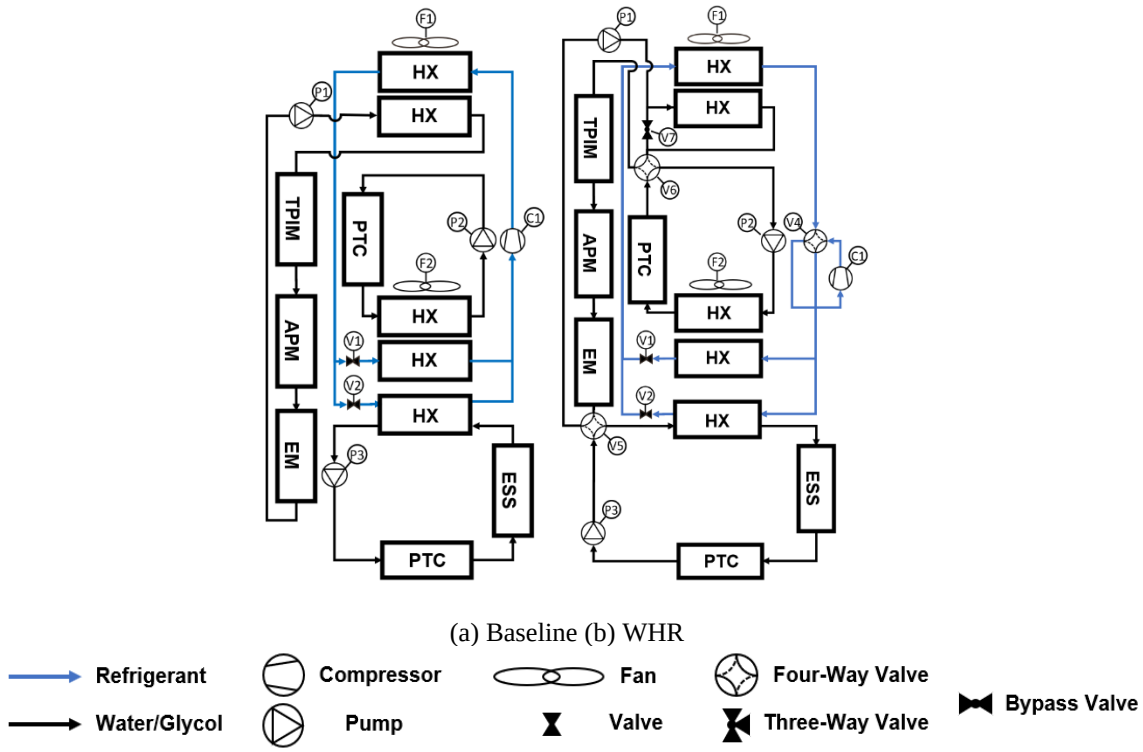

Figure 1: Schematic flow diagrams of all battery electric vehicle (BEV) integrated thermal management system (ITMS) architectures: (a) Baseline (Base), (b) Heat pump, PTC, and waste heat recovery (WHR)

2.2 Heat Pump, PTC, and Waste Heat Recovery (WHR) System

At the inlet to the TPIM in Figure 1b, the water glycol cools each of the electronic components and exits to a four-way valve (V5). This valve can either place the power electronics loop in series with the secondary loop for battery heating or maintain these as independent pumped loops. After either flowing through or bypassing the battery loop, the flow then passes to a second additional four-way valve (V6). This valve can similarly either place the power electronics in series with the cabin heating loop or bypass this cabin loop. Together, these valves allow waste heat from the power electronics to supplement necessary heating for the battery (V5) or cabin (V6). Finally, after either bypassing or flowing through the cabin heat exchanger, the water glycol flow comes to a simple bypass valve (V7) which plays a critical role in maintaining the temperatures of both the power electronics and the cabin environment. The valve operates to bypass the front-end radiator where the power electronics waste heat would typically be dumped to the environment if not being recovered.

Adding two more potential heat sources to control for the cabin inlet temperature in the architecture leads to three potential heat sources for controlling this variable at a given time, namely the cabin PTC, HP, and WHR systems. A layered control scheme is adopted from the CFL system investigated in the literature [4]. The control scheme works to use PTC power only when necessary during high demand periods. Once it falls below a threshold value of 50 W, compressor speed is controlled to ensure cabin conditioning. Finally, once the compressor speed falls below a threshold value of 5 Hz, the bypass valve then works to ensure the cabin inlet temperature by proportionally bypassing flow from the exchanger in a range of 0% to 100%. Additionally, the bypass valve operates to ensure the temperature of the power electronics. If at any point during heating operation the power electronics go above a safety threshold of 120 °C, the bypass engages to cool the power electronics over a 5 min period. This bypass mode, while available, is not typically engaged as the partial bypass flow for cabin heating regulates that either waste heat is being directed to the cabin or the environment in periods of low heating demand. Finally, the remaining control logic governs actuation of the four-way valves that place the water glycol loops into series or bypass modes. For the battery flow control valve (V5), the control variable is the mean temperature of the battery; once heated to a lower temperature threshold of 15 °C, the four-way valve actuates to bypass the battery. This removes the heating load of the battery and increases the available waste heating capacity for the cabin. The cabin four-way flow control valve (V6) is actuated based upon the

balance point temperature for system heating or cooling. In this way, whenever the ambient temperature is below the threshold of 20 °C waste heat is recovered to offset necessary electrical input.

3. SIMULATION METHODOLOGY, CONDITIONS, AND CASES

A transient modeling framework is adopted simulate all of the thermal, mechanical, and control volume systems in the systems using the Dymola modeling environment and written in the Modelica language [9]. This environment is multi-disciplinary, covering thermal, mechanical, electrical, and fluid flow systems with defined libraries of components. In this work, the TIL libraries are used to define thermal system components [10]. The modeling environment and specific details on each sub model are described in our previous work [8]. The following subsections outline the critical system modeling details, boundary and initialization conditions, including boundary conditions for the ambient and vehicle velocity. The transient initialization strategy is discussed in the context of system charge, pressure initialization, PI control initialization, and the initialization of the system as it transitions between heating and cooling mode. Finally, the simulation test cases to be examined across the different ITMS architectures are outlined.

3.1 System Modeling

Beginning first with the drive train model, a force balance on a theoretical vehicle is constructed accounting for forces including rolling resistance, drag, and vehicle inertia. Several key parameters such as mass of the system, drag, and rolling resistance coefficients, are assumed in the previous work [8], which then sets the total vehicle power requirements as a function of the input drive schedule. This then sets the power draw for the power electronics model.

The power electronics model is a black box model using singular constant efficiencies [8] to approximate both the power requirements experienced by each component and the total heat generation during a drive cycle. The power electronics include the electric machine or motor (EM), traction power inverter module (TPIM), and the auxiliary power module (APM). Each electronics component is parameterized as a heat source, adding heat to the liquid cooling loop defined in the baseline architecture via the TIL libraries [10]. The final power demand of the traction power inverter module is input to the battery model as an input variable, along with all other summed power demand in the system. Heat transfer calculations are calculated dynamically throughout the cycle run time by a set of heat transfer correlations implemented in heat exchanger models utilizing finite volume formulations [8].

The compressor modeled in this study (Emerson ZB21KCE-TFD) is selected to provide a target capacity of 6 kW of cooling at an ambient temperature of 35° C. This compressor speed is controlled with a proportional integral (PI)-controller based on an assumed maximum input taken from the compressor specifications.

$$\dot{m}_{comp} = \dot{m}_{map} \frac{N}{60} \tag{1}$$

$$\dot{W}_{comp} = \dot{W}_{map} \frac{N}{60} \tag{2}$$

Deviations from the performance mapping at superheat of 11.11K when simulating the system under transient operations are considered in the final governing equations for the compressor model by setting the factor F to 0.75 in the following corrections:

$$\dot{m}_{new} = \dot{m}_{comp} \left(1 + F \cdot \left(\frac{\rho_{suc,new}}{\rho_{suc,data}} - 1\right)\right) \tag{4}$$

$$\dot{W}_{new} = \dot{W}_{comp} \left(\frac{\dot{m}_{new}}{\dot{m}_{comp}} \cdot \frac{\Delta h_{s,new}}{\Delta h_{s,map}}\right) \tag{5}$$

It is further assumed that the compressor work is transferred to the refrigerant to fix the outlet state. From the VCC, heat is extracted from the air recirculating from the cabin, mixing with fresh ventilated air from the ambient environment. The cabin environment is parameterized via inside and outside heat transfer coefficients which account for natural convection in the cabin environment and velocity driven airflow across the outside of the cabin with the addition of constant solar flux.

3.2 Boundary Conditions

For the purposes of this study, fixed conditions are assumed with the vehicle driving north with no wind on a clear sunny day, at constant ambient temperature, humidity, and the resulting air psychrometric properties. The vehicle cabin is exposed to direct and diffuse solar radiation of 600 and 200 W/m^2, respectively. The constant ambient temperature is varied parametrically between each case across a range of -20 °C to 40 °C. The vehicles velocity schedule is defined by the time varying input of a multi-cycle test (MCT) [11] methodology, as described in detail in the preceding work [8]. This drive cycle provides benefit for simulation time as well leading to shortened simulation time overall.

3.3 Initialization Conditions

Initialization conditions must be specified to form a well posed problem to be solved numerically. The initial conditions include pressure and temperature initialization for the VCC equipment and fluid, temperature initialization conditions for solid thermal masses in the system, and initial temperature for the cabin volume. For the VCC, low- and high-side pressures of the compressor are initialized at 500 kPa and 1200 kPa, respectively, for all simulations across heating and cooling modes. For the purposes of this simulation the system charge is set to 0.75 kg. A soak initialization condition is chosen such that the thermal masses inside of the system are initialized at the ambient temperature for the test condition. The battery is initially charged to SOC = 0.95 with an initial current of zero. For the water glycol circulating loops the PI controls are initialized at 0.25 kg/s while the compressor and mass flow through the VCC system are initially shutoff.

3.4 Simulation Cases

Test cases are performed at fixed ambient temperatures of -20 °C, -10 °C, 0 °C, 10 °C, 25 °C, 30 °C, and 40 °C. At each ambient temperature, the cabin setpoint is evaluated at 18 °C, 20 °C, 22 °C, and 24 °C. The cabin setpoints determine the heating or cooling targets of the system across the simulated MCT cycle. During heating simulation cases the battery setpoint is 15 °C and during cooling cases the battery is set to 35 °C.

4. RESULTS

With the modeling methodology, thermal system architectures, and boundary conditions established, the two thermal management systems are simulated across the MCT cycle. This allows for comparisons of driving range across parameters of the thermal management system, ambient temperature, and cabin setpoint temperature. Finally, a transient cycle for the WHR system of most interest is examined across a MCT simulation, highlighting the heat transfer and control setpoints during transient performance.

4.1 Comparison of Driving Ranges

The bar charts presented in Figure 2 show the system ranges across the range of ambient temperatures at each cabin setpoint temperature. Clear trends are observed in system performance as the cabin setpoint varies across the range of ambient temperatures. On average, for both architectures in most stringent cooling mode (i.e., ambient of 40 °C). the projected range for the system decreases by approximately 2-3% for every 2 °C reduction in the cabin setpoint from 24 °C to 18 °C. This leads to an overall variation of 12% in driving range for the baseline system depending on the user-determined cabin set point. Under the ambient temperature range that demands cabin heating (from -20 °C to 10 °C), the two architectures become more distinct in their performance. Compared to the cooling demands, these heating cases having more severe impact on driving range that justifies a focus on exploring architecture improvements for heating efficiency. Beginning with a general assessment, an overall decrease in the max range of 32.9 to 38.9%, depending on the cabin setpoint temperature, is experienced by the baseline system as the ambient temperature is reduced to -20 °C. This amounts to a total range reduction of 80 to 100 miles for the baseline system.

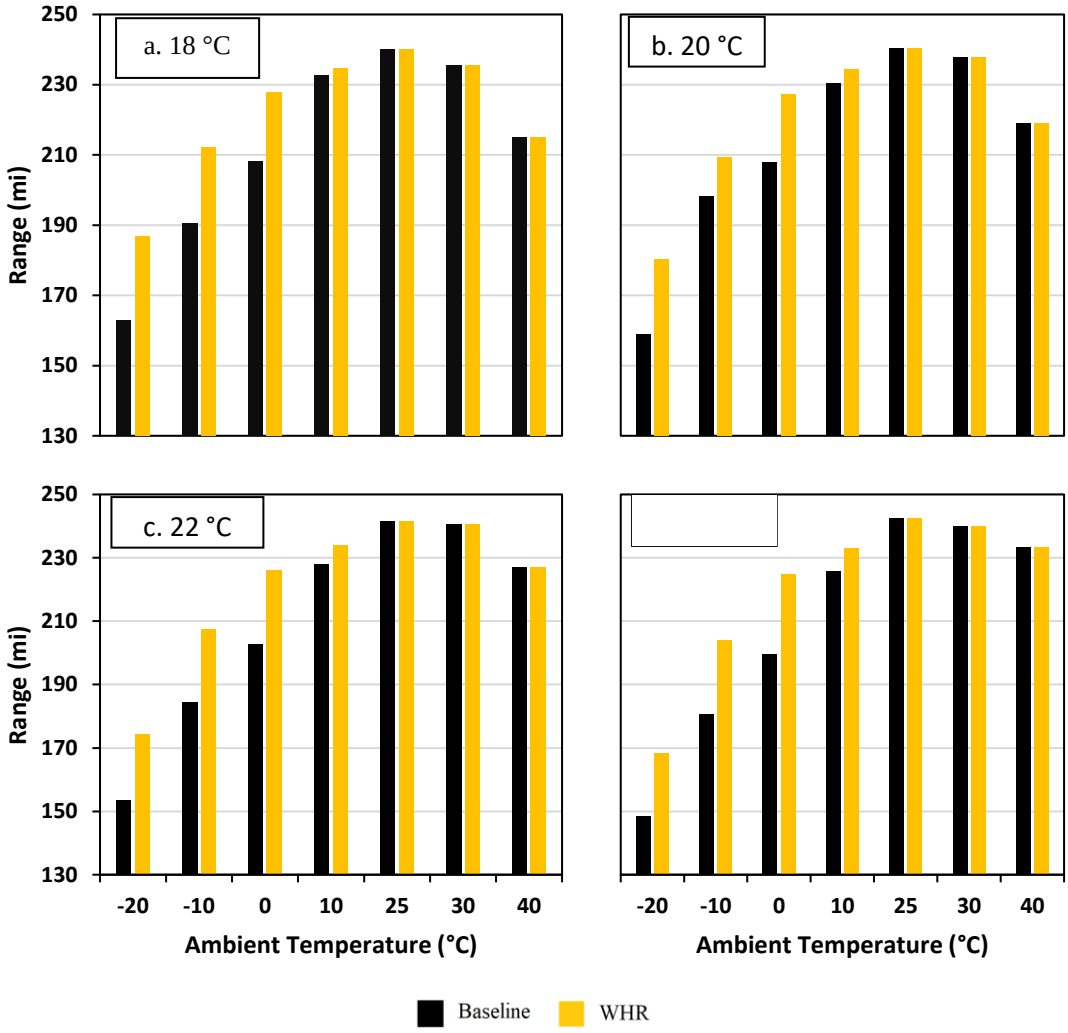

Figure 2: Simulated driving ranges for the two different ITMS architectures (Baseline, WHR) across a parametric variation in ambient temperature (-20 °C, -10 °C, 0 °C, 10 °C, 25 °C, and 30 °C) at cabin setpoints of: a. 18 °C, b. 20 °C, c. 22 °C, and d. 24 °C.

With the baseline use of water glycol loops for cabin and battery conditioning, the WHR architecture was established to allow heat scavenging from the electronics cooling loop. The WHR system provides clear advantages at lower ambient temperatures (0 °C to -20 °C). At these temperatures, the system experiences a further increase in effective range owing to the utilization of waste heat. At the 0 °C ambient condition, an increase of 10% in driving range is gained as compared to the baseline system. This increase is then accentuated at -10 °C and -20 °C test conditions, for which the compressor in the heat pump cannot provide all the heating load necessary for the cabin. At these ambient temperatures, the WHR system can supplement the necessary cabin heating requirements, which leads to the relative increase in range as compared to the baseline system. This increase is large at the -20 °C condition as a larger portion of electric heating is needed to meet the demand in the baseline system compared to the WHR system while the steady state demand of the WHR system can be completely supplemented by heat pump and WHR operation. The next section will further discuss the transient response of the WHR system to illustrate the reduced electric heating load due to recovered heat from the power electronics.

4.2 Transient ITMS Response

Shown in Figure 3 is a plot of the transient compressor power, PTC heater power, and cabin HX throughout the drive cycle for the WHR architecture simulated at an ambient temperature of -10 °C, a cabin setpoint of 24 °C, and a battery setpoint of 15 °C. Several features of the control logic are illustrated in this plot. First, from the initialized soak condition, the electric heater for the cabin is set to a maximum of 6 kW of power. A clear gap in heating performance is observed between 0 s and when the cabin then reaches its setpoint at ~1400 s. The 6 kW of power for the electric heater appears to not be transferred to the cabin HX. This is due to the orientation and layout of the flow control systems in the WHR architecture, the thermal mass of the battery, and the size of the battery heater itself. Its observed from Figure 1b that the cabin PTC heater flows into the battery which extracts heat before the cabin HX, effectively delaying the heating action of the cabin which can be seen completes at 1400 s in the transient plot, at which point the PTC heater begins to adjust to control the inlet cabin temperature while the system actuates the inlet volume flow rate. A corresponding dip in battery heating can be observed. In this way, the sizing of the battery heater, the orientation of the flow systems, and the battery thermal mass can have significant deleterious effects on the cabin heating performance which are clearly demonstrated.

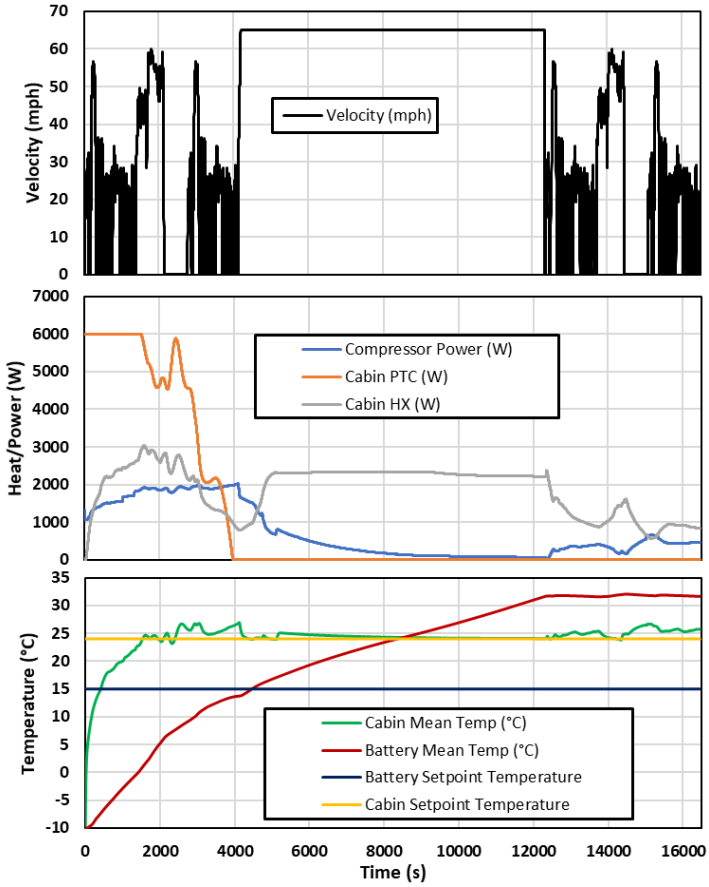

Figure 3: (a) Simulated MCT drive cycle. The simulated heat loads and power draws throughout the cycle time are plotted for: (b) the heat exchange in the WHR architecture at -10 °C ambient with a 24 °C cabin and 15 °C battery setpoints; and (c) the setpoints of the WHR architecture at -20 °C ambient with a 24 °C cabin and 15 °C battery setpoints

At this point, from 1700 s to 2600 s, the flow rate into the system initially decreases as the cabin setpoint is surpassed and, due to slight fluctuations in PI control, dips briefly below its setpoint until settling at the control point as the fan volume flow rate decreases. Eventually, at ~4000 s, the electric heater completely shuts off while the cabin HX and compressor power completely compensate for the necessary steady state heating load of the system. As time progresses, during the high constant speed portion of the cycle, the WHR supplements most of the heating load, allowing the compressor to essentially shut off. After this constant speed portion, at ~12000 s, the system enters a mixed control condition where the compressor controls the cabin inlet temperature while the power electronics radiator

is completely bypassed. Overall, this control scheme and architecture meets the necessary EV setpoint temperatures while extending system range via the utilization of waste heat. Compared to the baseline, this flow control is enabled through the addition of a four-way valve (V4) to allow operation of the VCC as a heat pump and two four-way valves (V5 and V6) actuated to allow waste heat recovery. Implications on future work and system implementation are clear, as this result demonstrates the need for study on effective and flexible flow configuration, as well as the benefits of battery and cabin pre-heating.

5. CONCLUSIONS

This work performed an investigation of integrated thermal management systems (ITMS) for long-range battery electric vehicles, specifically comparing a baseline long range EV system to a system having provisions for waste heat recovery meant to improve system operation and performance in cold climates. This involved the setup of a comprehensive dynamic model to evaluate the range performance across various thermal systems architectures. The impacts on range of cabin thermal management are clearly enumerated with the impacts of the large thermal masses of the battery and cabin quantified in a transient simulation of mixed control schemes. These have broad implications for the optimal thermal management system for long-range EV's. Several key conclusions are drawn regarding long-range BEV thermal system performance:

- The inclusion of the battery as a necessary heating mass places a burden upon combined WHR systems that require further system optimization.
- The advantages of the WHR system are shown when examining the components necessary to enable its advantages; namely only the addition of three four-way, flow reversing valves and the use of a common heat transfer fluid, water glycol.
- WHR systems provide unique benefits for these long-range systems depending on the drive schedule enabled by their long-range operation.

REFERENCES

[1] J. Kim, J. Oh and H. Lee, "Review on battery thermal management system for electric vehicles," *Applied Thermal Engineering,* vol. 149, pp. 192-212, 2018.

[2] M. Al-Zareer, I. Dincer and M. A. Rosen, "A review of novel thermal management systems for batteries," *International Journal of Energy Research,* vol. 42, no. 10, pp. 3182-3205, 2018.

[3] Z. Zhang, J. Wang, X. Feng, L. Chang, Y. Chen and X. Wang, "The solutions to electric vehicle air conditioning systems: A review," *Renewable and Sustainable Energy Reviews,* vol. 91, pp. 443-463, 2018.

[4] G. Titov and J. Lustbader, "Modeling control strategies and range impacts for electric vehicle integrated thermal management systems with MATLAB/Simulink," *SAE Technical Paper,* no. 2017-01-0191, 2017.

[5] A. Carriero, M. Locatelli, K. Ramakrishnan, G. Mastinu and M. Gobbi, "A review of the state of the art of electric traction motors cooling techniques," *SAE Technical Paper,* no. 2018-01-0057, 2018.

[6] K. J. Kelly, T. Abraham, K. Bennion, D. Bharathan, S. Narumanchi and M. O'Keefe, "Assessment of thermal control technologies for cooling electric vehicle power electronics," in *23rd International Electric Vehicle Symposium (EVS-23),* Anaheim, 2007.

[7] A. Bhunia, S. Chandrasekaran and C.-L. Chen, "Performance improvement of a power conversion module by liquid micro-jet impingement cooling," *IEEE Transactions on Components and Packaging Technologies,* vol. 30, no. 3, pp. 309-316, 2007.

[8] T. J. Shelly, J. A. Weibel, D. Ziviani and E. A. Groll, "A Dynamic Simulation Framework for the Analysis of Battery Electric Vehicle Thermal Management Systems," in *19th IEEE Intersociety Conference on Thermal and Thermomechanical Phenomena in Electronic Systems (ITherm),* Orlando, 2020.

[9] S. E. Mattsson and H. Elmqvist, "Modelica - An International Effort to Design the Next Generation Modeling Language," *IFAC Proceedings Volumes,* vol. 30, no. 4, pp. 151-155, 1997.

[10] TLK-Thermo GmbH, "TLK-Thermo – Engineering Services and Software for Thermal Systems," TLK-Thermo GmbH, [Online]. Available: https://www.tlk-thermo.com/index.php/en/. [Accessed 07 1 2020].

[11] SAE, *Surface vehicle reccomended practice: Battery Electric Vehicle Energy Consumption and Range Test Procedure,* 2017.

ACKNOWLEDGEMENT

Financial support for this work provided by members of the Cooling Technologies Research Center is gratefully acknowledged. The authors would like to acknowledge members of the Technical University of Braunschweig, Michael Steeb and Ingo Frohböse, for their support in providing access to the Modelica libraries.